International Journal of Biological Macromolecules 192 (2021) 1344–1356

Contents lists available at ScienceDirect

International Journal of Biological Macromolecules

journal homepage: www.elsevier.com/locate/ijbiomac

Photocrosslinkable gelatin/collagen based bioinspired polyurethane-acrylate bone adhesives with biocompatibility and biodegradability

Sevgi Balcioglu [a,*], Canbolat Gurses [b], Imren Ozcan [c], Azibe Yildiz [d], Suleyman Koytepe [c], Hakan Parlakpinar [e], Nigar Vardi [d], Burhan Ates [c,**]

[a] Sakarya University of Applied Sciences, Department of Medicinal Laboratory, Sakarya, Turkey
[b] İnönü University, Science Faculty, Department of Molecular Biology and Genetics, Malatya, Turkey
[c] İnönü University, Science Faculty, Department of Chemistry, Malatya, Turkey
[d] İnönü University, Medical Faculty, Department of Histology and Embryology, Malatya, Turkey
[e] İnönü University, Medical Faculty, Department of Medicinal Pharmacology, Malatya, Turkey

ARTICLE INFO

Keywords:
Bone adhesive
Polyurethane-acrylate
Gelatin, collagen, UV-curing
Antibacterial activity
Biodegradability
Flexibility
Biocompatibility

ABSTRACT

Hard or soft tissue adhesives have been presented as a promising candidate to replace traditional wound closure methods. However, there are mechanical strength problems in biological adhesives and biocompatibility problems in synthetic-based adhesives. At this point, we aimed to remove all these disadvantages and produce a single adhesive that contains all the necessary features and acrylate functionalized UV-curable polyurethane formulations were produced with high crosslink density, high adhesion strength, biocompatibility and injectable property for easy application as potential biomedical adhesives. Aliphatic isophorone diisocyanate (IPDI) was used as the isocyanate source and β-cyclodextrin was used for host-guest relationship with gentamicin by crosslinking. Proteins (gelatin (GEL), collagen (COL)) and PEGs of various molecular weight ranges (P200, P400, P600) were selected as the polyol backbone for polyurethane synthesis due to their multiple biological activities such as biocompatibility, biodegradability, biomimetic property. Several techniques have been used to characterize the structural, thermal, morphological, and various other physicochemical properties of the adhesive formulations. Besides, the possibility of its use as a hard tissue adhesive was investigated by evaluating the tissue adhesion strength *in vitro* and *ex vivo via* a universal testing analyzer in tensile mode. Corresponding adhesive formulations were evaluated by *in vitro* and *in vivo* techniques for biocompatibility. The best adhesion strength results were obtained as 3821.0 ± 214.9, and 3722.2 ± 486.8 kPa, for IPDI-COL-P200 and IPDI-GEL-P200, respectively. Good antibacterial activity capability toward *Escherichia coli Pseudomonas aeruginosa*, and *Staphylococcus aureus* were confirmed using disc diffusion method. Moreover, cell viability assay demonstrated that the formulations have no significant cytotoxicity on the L929 fibroblast cells. Most importantly, we finally performed the *in vivo* biodegradability and *in vivo* biocompatibility evaluations of the adhesive formulations on rat model. Considering their excellent cell/tissue viability, fast curable, strong adhesion, high antibacterial character, and injectability, these adhesive formulations have significant potential for tissue engineering applications.

1. Introduction

In recent years, more and more attention of researchers on soft and hard tissue adhesives as an alternative to traditional wound closure and bone fixation applications has increased due to their numerous advantages such as better comfort and lower cost [1,2]. Additionally, unlike sutures and staples they are the most suitable non-invasive method for gluing surfaces together [3,4]. The fibrin sealants and cyanoacrylate adhesives have been used extensively in biomedical applications for sealing and bonding purposes [3,5]. Fibrin adhesives have

* Correspondence to: S. Balcioglu, Sakarya University of Applied Sciences, Vocational School of Health Services at Akyazı, Department of Medical Services and Techniques, Sakarya, Turkey.
** Corresponding author.
E-mail addresses: sevgibalcioglu@subu.edu.tr (S. Balcioglu), burhan.ates@inonu.edu.tr (B. Ates).

https://doi.org/10.1016/j.ijbiomac.2021.09.043
Received 10 June 2021; Received in revised form 30 August 2021; Accepted 8 September 2021
Available online 15 September 2021

high biocompatibility, but their mechanical performance is poor due to the lack of protein-protein crosslinking. [3] On the other hand, adhesives based on cyanoacrylate form strong bonds through free radical polymerization while exhibiting poor biocompatibility [6,7]. Therefore, in order to overcome these limitations, it is essential to develop a new adhesive formulation that is molecularly adjustable, shows high mechanical and adhesion strength and good biocompatibility.

Nowadays, satisfactory results can be obtained when UV-curing technology is applied in adhesives [8–10]. This technology has been considered superior to thermal curing due to its eco-compatible process and excellent properties resulting from high crosslink density [8]. Especially, multifunctional acrylates such as polyurethane acrylates have been widely used as UV-curable adhesives because of its excellent flexibility, exceptional adhesion on substrates, superior impact resistances and short curing time (~3–5 min) [11–13]. However, due to their poor thermo-mechanical stability [14] the crosslinking of multifunctional acrylates is required to improve accordingly [15].

At this point, we hypothesized that acrylate functionalized UV-curable polyurethane formulations can be produced with high crosslink density, high adhesion strength, biocompatibility and injectable property for easy application as potential biomedical adhesives. This mechanism also can be combined with covalent modification and crosslinking of proteins to obtain effective and biocompatible adhesive formulations. For instance, collagen (COL) is the primary and most abundant structural protein found in mammal bodies which comprise about 25–30% of the whole-body protein content [16]. It is an appropriate material for tissue healing applications because of high biocompatibility, biodegradability, low immunogenicity, and inductivity for tissue healing [17]. Furthermore, it is widely used in musculoskeletal tissue engineering applications due to its superior properties such as porous structure and good permeability [18]. However, the biggest handicap of COL-based materials is their insufficient mechanical strength, which prevents their application in soft tissue regeneration [17]. On the other hand, gelatin (GEL) is a protein-based polymer obtained from COL degradation. It exhibits proven exceptional biocompatibility, biodegradability, weak immunogenicity [18,19]. Besides, it improves cell surface adhesion due to having bioactive motifs (L-arginine, glycine, and L-aspartic acid (RGD) peptides) [18,20].

Our previous research on the development of soft tissue adhesives focused on the use of natural saccharide-based polyurethane such as maltose [21], sucrose [21], and xylose [22] to apply for surgical operations. Although the adhesive materials were shown flexibility due to the PEG group, they were confirmed to have high strength when by cover a crosslinking on metal substrates. Besides, by combining chlorogenic acid containing mussel-inspired catechol groups, we produced a strong, flexible, and tunable adhesive [23]. In addition, we also demonstrated the tunability of our adhesives for moist tissues, which is an advantage in terms of mechanical stability during bonding. For this purpose, we reported that the molecular design of Tween units with hydrophobic moieties displayed the strong adhesion of the formulations under wet conditions [24].

Compared to the previous studies, here, we focused on the design, synthesis and characterization of acrylate functionalized UV-curable polyurethane formulations as potential biomedical adhesives. Chemically functionalizing the polyurethane polymers with acrylate also provides an appropriate way to control the UV-curing and simplifies adhesion time and application because of the injectable form. Also, using of dopamine methacrylamide in UV-curing process provides a mussel-mimetic curing mechanism as well as curing by opening the double bond thanks to the catechol functional groups it contains. The adhesive formulations' chemical structure, thermal behavior, microstructure, topographic surface, gentamicin release property, adhesion strength, protein adsorption, antibacterial activity and biodegradation abilities were evaluated *in vitro* and bone adhesion strengths were evaluated *ex vivo*. Moreover, we determined the cytotoxic properties of the adhesive formulations using the MTT assay, which also shows the cell compatibility of our materials. Finally, we confirmed the *in vivo* biocompatibility and biodegradation of our adhesive formulations through a rat model to evaluate the immune response to the adhesive formulations.

2. Experimental section

2.1. Materials

Isophorone diisocyanate (IPDI) (98%), collagen (COL) from bovine achilles tendon, gelatin (GEL) from porcine skin, 2-Isocyanatoethyl methacrylate (98%), Irgacure-2959 (98%) were purchased from Sigma-Aldrich. PEGs (PEG200 (190–210 g/mol), PEG400 (380–420 g/mol) and PEG600 (570–630 g/mol)), and β-Cyclodextrin (>99.0%) were acquired from Merck and TCI, respectively. In cell culture, Dulbecco's modified Eagle's medium (DMEM), Fetal bovine serum (FBS), penicillin/streptomycin, and thiazolyl blue tetrazolium bromide were obtained from Sigma-Aldrich. A commercialized cyanoacrylate adhesive was purchased from VenaBlock. Phosphate-buffered saline (PBS, pH 7.4) was obtained from BioShop. All chemical agents were used as received without further purification.

2.2. Synthesis of pre-polyurethanes

In current study, the polymer synthesis was carried out in two steps. The first step was the synthesis of polyurethane containing free hydroxyl (-OH) groups (pre-polyurethane), and the second one was the synthesis of acrylate end groups of pre-polymers.

For pre-polyurethane synthesis, IPDI, β-cyclodextrin, proteins (GEL and COL), and PEGs with different molecular weights (PEG200, PEG400 and PEG600) were stoichiometrically added into a Schlenk flask at the ratios indicated in Table 1. In formulations, only one protein (GEL or COL) was used as a protein source, whereas in formulations containing PEG only one of the selected PEGs was added. The products were named as pre-polyurethane (Fig. 1). The reaction was refluxed in DMSO at 75 °C under argon atmosphere for 24 h and catalyzed by triethylamine. The success of the synthesis was followed by FTIR and the reaction was terminated when there was no free isocyanate peak. The NCO/OH ratio in the reaction was theoretically adjusted to be 1/1.2, 1/1.3, and 1/1.4 to provide free hydroxyl groups (20, 30 and 40, respectively as stoichiometrically).

2.3. Preparation of acrylate functionalized pre-polymers

After determining the number of free -OH groups according to ASTM E1899-08 potentiometric titration standard method of the synthesized polyurethanes, 2-isocyanatoethyl methacrylate was stoichiometrically added to the reaction solution with the same ratio of free hydroxyl groups in DMSO medium. The reaction was carried out in an inert atmosphere for 6 h at room temperature. The synthesis was followed by FTIR and the reaction was terminated with the disappearance of the free isocyanate peak at 2265 cm^{-1}. Acrylate functionalized polymers obtained at this stage were named as pre-polymer (Fig. 1 and Table 1). We named pre-polymers by adding the letter A (represents acrylate) to the end of their pre-polyurethane names such as IPDI-GEL-P200-20-A.

2.4. Gentamicin loading

Gentamicin, a systemic antibiotic, was used for the antibacterial behavior of the prepared pre-polymers. The amount of gentamicin was adjusted so that its final concentration in the bioadhesive was 2.5% by weight. This concentration was reported as the most effective dose in a study on bone cement [25]. It was stirred at room temperature for 2 h to homogenously distribute gentamicin into the polymer solution and complete the host-guest interaction with the β-cyclodextrin (Fig. 1). After adding gentamicin, the samples were dried overnight under

Table 1
The compositions of the polymers.

Pre-polyurethane	IPDI	PEG	Protein	B-cyclodextrin	Pre-polymer	Polyurethane-acrylate
IPDI-GEL-P200-20	100	P200/105	GEL/5	10	IPDI-GEL-P200-20-A	IPDI-GEL-P200-20-AC
IPDI-GEL-P200-30	100	P200/115	GEL/5	10	IPDI-GEL-P200-30-A	IPDI-GEL-P200-30-AC
IPDI-GEL-P200-40	100	P200/125	GEL/5	10	IPDI-GEL-P200-40-A	IPDI-GEL-P200-40-AC
IPDI-GEL-P400-20	100	P400/105	GEL/5	10	IPDI-GEL-P400-20-A	IPDI-GEL-P400-20-AC
IPDI-GEL-P400-30	100	P400/115	GEL/5	10	IPDI-GEL-P400-30-A	IPDI-GEL-P400-30-AC
IPDI-GEL-P400-40	100	P400/125	GEL/5	10	IPDI-GEL-P400-40-A	IPDI-GEL-P400-40-AC
IPDI-GEL-P600-20	100	P600/105	GEL/5	10	IPDI-GEL-P600-20-A	IPDI-GEL-P600-20-AC
IPDI-GEL-P600-30	100	P600/115	GEL/5	10	IPDI-GEL-P600-30-A	IPDI-GEL-P600-30-AC
IPDI-GEL-P600-40	100	P600/125	GEL/5	10	IPDI-GEL-P600-40-A	IPDI-GEL-P600-40-AC
IPDI-COL-P200-20	100	P200/105	COL/5	10	IPDI-COL-P200-20-A	IPDI-COL-P200-20-AC
IPDI-COL-P200-30	100	P200/115	COL/5	10	IPDI-COL-P200-30-A	IPDI-COL-P200-30-AC
IPDI-COL-P200-40	100	P200/125	COL/5	10	IPDI-COL-P200-40-A	IPDI-COL-P200-40-AC
IPDI-COL-P400-20	100	P400/105	COL/5	10	IPDI-COL-P400-20-A	IPDI-COL-P400-20-AC
IPDI-COL-P400-30	100	P400/115	COL/5	10	IPDI-COL-P400-30-A	IPDI-COL-P400-30-AC
IPDI-COL-P400-40	100	P400/125	COL/5	10	IPDI-COL-P400-40-A	IPDI-COL-P400-40-AC
IPDI-COL-P600-20	100	P600/105	COL/5	10	IPDI-COL-P600-20-A	IPDI-COL-P600-20-AC
IPDI-COL-P600-30	100	P600/115	COL/5	10	IPDI-COL-P600-30-A	IPDI-COL-P600-30-AC
IPDI-COL-P600-40	100	P600/125	COL/5	10	IPDI-COL-P600-40-A	IPDI-COL-P600-40-AC

vacuum.

2.5. UV-curing process

For the curing process, 1 g of the pre-polymers were dissolved in 500 μL absolute ethanol. Meanwhile, 10 mg of photoinitiator and 10 mg of dopamine methacrylamide were dissolved in 50 μL of absolute ethanol and the mixture was transferred into pre-polymers solution. Afterward, the final mixture was exposed to UV light for 5 min until the components were completely cured (Fig. 1). The optimum curing time was determined by adhesion tests. Different curing times were tried up to 15 min and maximum adhesion strength was reached in the 5th minute. Irgacure D-2959 was used as the photoinitiator (365 nm, 8 w/cm^2 and 30 cm from the material). The reason for using dopamine methacrylamide in UV-curing processes is to provide a mussel-mimetic curing mechanism as well as curing by opening the double bond thanks to the catechol functional groups it contains. Thus, the samples were cured faster by two different mechanisms. At the end of curing, a solid, reticulated, insoluble, transparent polymer was obtained and named as polyurethane-acrylate (Table 1). We named polyurethane-acrylates by adding the letter AC (represents cured-acrylate) to the end of their pre-polymer names such as IPDI-GEL-P200-20-AC.

2.6. Structural, thermal and morphological characterization

FTIR (Perkin Elmer) was used to determine the functional groups of all synthesized adhesive formulations. The FTIR spectra were recorded in the 400–4000 cm^{-1} range. ^{1}H NMR spectra were recorded on a Bruker Ascend™ 400 Avance at room temperature. Thermogravimetric analysis (TGA), differential scanning calorimetry (DSC) and differential thermal analysis (DTA) techniques were used to determine the thermal behavior and glass transition temperatures (Tg) of samples before and after UV-curing. TGA (Shimadzu TGA-50) and DTA (Shimadzu DTA-50) analysis was performed from 25 to 600 °C under air atmosphere at a heating rate of 10 °C min^{-1}. DSC (Shimadzu DSC-60) analysis was carried out from −40 to 100 °C at a heating rate of 10 °C min^{-1}. The samples were cooled by liquid nitrogen for DSC analysis. Scanning electron microscopy (SEM, LEO Evo-40 VPX) and atomic force microscopy (AFM, XE-100E; Park Systems Corp., Suwon, Korea) analysis was performed on the selected samples to determine the general morphological structures of the final polymer formulations after UV-curing.

2.7. Determination of adhesion strength and ex vivo testing

ASTM (F2255-03, Test method for strength properties of tissue adhesives in lap-shear by tension loading) standard test was performed to determine the adhesion strength analysis of the synthesized adhesives. The measurements were carried out by placing the two glass slides on top of each other in a specific area and then applying a tensile test (lap shear adhesion test) with a mechanic test analyzer (MTS Exceed Series Model E42 Test System). First, 50 mg of pre-polymer sample was dissolved in 25 μL of absolute ethanol for better spreadability. In another tube, a mixture containing 0.5 mg of Irgacure D-2959 and 0.5 mg of dopamine methacrylamide was prepared in 2.5 μL of absolute ethanol. Afterward, all the components were applied to an area of 2.5 × 1 cm^2 of the glass slide and lightly combined with the other glass slide. The dual glass slide system was then exposed to UV light for 15 min. The pre-polymers prepared thanks to the transparent character of the glass slides were cured rapidly. The adhesion strength was determined by pulling the glass slides at a speed of 50 mm/min. The experiments were performed at least three times and the results were presented as kPa.

Ex vivo compression test of the adhesives was carried out with bone tissue taken from the bovine rib area. The photographs of the application of the compression strength studies are presented in Fig. 4(A–F). In the test, the bone tissue (Fig. 4A) was cut in appropriate forms and applied between the adhesives prepared and cured with UV (Fig. 4B, C, and D). Then, the bone tissue was placed in the mechanical test analyzer as seen in Fig. 4E. The apparatus to perform the compression test applied pressure on the bone with a speed of 0.02 mm/s and the compressive strength of the adhesives was measured (Fig. 4F). Experiments were carried out at least three times.

2.8. In vitro hydrolytic biodegradability, in vitro gentamicin release and antibacterial activity

To examine the *in vitro* hydrolytic biodegradability of the adhesive formulations, the film samples were cut into 1 × 1 cm^2 diameter pieces and weighed (W_0). The weighed samples were immersed in 5 mL of PBS (pH: 7.4, 50 mM) and incubated at 37 °C for 4 weeks. The samples were withdrawn at 1, 2, 3, and 4 weeks, washed with PBS, and dried. The dried samples were reweighed (W_1). The weight loss (%) was calculated by using the formula below.

$$\text{Weight loss } (\%) = \frac{W0 - W1}{W0} \times 100$$

To examine the gentamicin release kinetic, 0.1 g of the samples were immersed in 10 mL of PBS (pH:7.4, 50 mM) and incubated at 37 °C over a period up to 5 days. The release medium was collected at certain time intervals (0.25, 0.5, 1, 2, 4, 24, 48, 96, and 120 h) and PBS was restored with fresh one at each withdrawal. The release medium was passed through a membrane filter (pore size 0.45 μm). The amount of gentamicin released was determined by derivatizing with o-phthalaldehyde

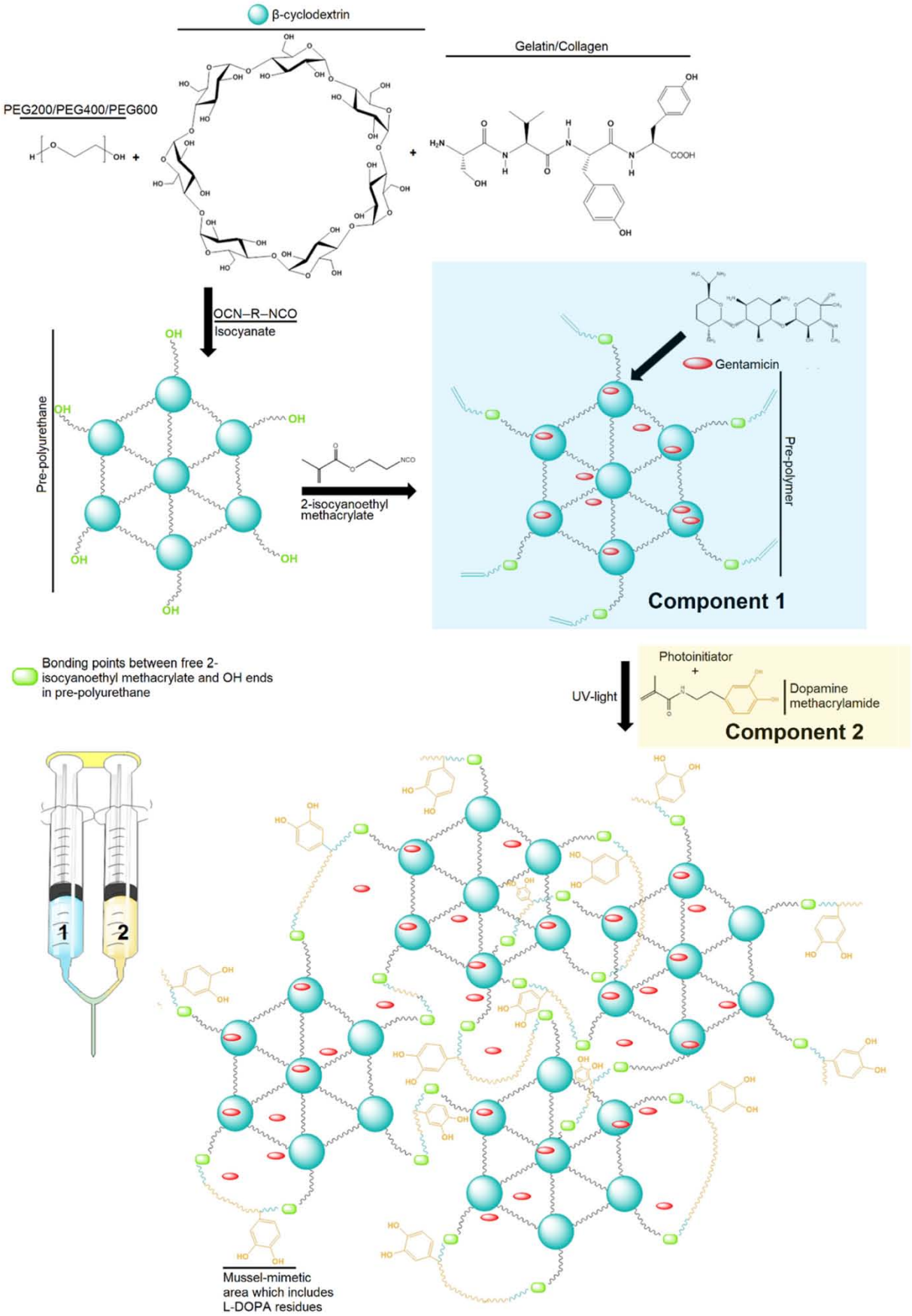

Fig. 1. Schematic representation of the monomer design and synthesis of pre-polyurethane and pre-polymers followed by UV-curing of the pre-polymer with dopamine methacrylamide during the application.

(OPA) and measuring the absorbance of the complex formed at 340 nm [26]. Gentamicin concentration was calculated by using the standard calibration plot of gentamicin sulfate. The measurements were repeated on at least three independent samples.

The agar disc diffusion method [27] was used to determine the antimicrobial effects of the adhesive formulations. The microorganisms used for the test were *Escherichia coli* (*E. coli* ATCC 25922; Gram-negative), *Pseudomonas aeruginosa* (*P. aeruginosa* ATCC 27853; Gram-negative) and *Staphylococcus aureus* (*S. aureus* ATCC 23235; Gram-positive). While Luria-Bertani broth was prepared for optimum growth of *E. coli* and *P. aeruginosa*, tryptic strain broth was prepared for *S. aureus*. The adhesive formulations were cut into small discs (0.5 cm diameter). A filter paper disc was spotted with gentamicin solution containing 1.25 mg gentamicin to prepare a positive control. All samples were sterilized with UV for 30 min before being used.

2.9. Protein adsorption

For the protein adsorption test, 0.1 g of the adhesive formulations were soaked in 5 mL solution containing 0.32 mg/mL BSA and 0.03 mg/mL fibrinogen for adsorption for 16 h and 3 h, respectively. The samples were then removed from the protein solutions and washed twice with PBS. After adsorption, the adhered proteins were re-transferred to the solution by mixing 1 mL of 1% SDS solution for 3 h. The amount of protein taken into the solution was measured at 340 nm using OPA derivatization [22]. The amount of protein adsorbed was calculated as μg protein/0.1 g polymer.

2.10. In vitro biocompatibility

Cell viability values of adhesive formulations were determined spectrophotometrically by using MTT test with indirect method. ISO-10993-5 (Biological Evaluation of Medical Devices) standard experimental protocol was applied using *Mus musculus* type mouse fibroblast cells (L-929). First, the samples were washed with sterile PBS (pH 7.4), sterilized under UV light for 1 h and incubated with DMEM medium in an oven containing 5% CO_2 at 37 °C for 72 h. For the experiment, the L-929 cell line was grown in DMEM medium at 37 °C in an oven containing 5% CO_2 until 80% confluent, then the cells were removed from the flasks with 0.25% trypsin-EDTA solution. The cells taken by centrifugation at 2000 rpm for 5 min were then planted in 96-well plates at 10^4 cells/well and incubated under the same conditions for 24 h. After incubation, the supernatant medium of each well was replaced with 90 μL of fresh DMEM solution. 10 μL of MTT solution (5 mg/mL PBS) was then added and incubated in the dark for 4 h at 37 °C. The optical density of the resulting solution was measured by using a microplate reader (Biotek, USA) at 550 nm. Cell viability was calculated as a percentage in relation to the control group, taken as 100%. Furthermore, confluent rates (%) were presented by determining cell morphologies with JuliFL cell analyzer.

2.11. In vivo biocompatibility

In vivo biocompatibility evaluation of the formulations was carried out at Inonu University Experimental Animal Production and Research Center with the number of 2016/A-27 according to ethical use protocols of rats. Based on the results of *in vitro* biocompatibility tests, the most suitable two adhesive formulations were used in *in vivo* biocompatibility experiments. The *in vivo* biocompatibility test was carried out in two stages, acute (one week) and chronic (four weeks). In the experiment, 36 male adult Wistar rats were first anesthetized with urethane and divided into groups such that two identical specimens were implanted in the right and left dorsal area of each animal. The samples prepared with a diameter of 1 × 1 cm^2 were sterilized for 1 h in ethyl alcohol (70% v/v) and 1 h under UV light, respectively. Then the right and left dorsal areas of the animals were incised, two independent sample implanted and the area was sutured with surgical suture. SUPERSTOCK 1012P clear polypropylene samples (PP) were implanted in animals as positive controls. The animals were kept alive in their normal life cycle and were sacrificed under anesthesia at the end of the 1st and 4th weeks. Histological and biochemical characterizations were evaluated by taking the muscle tissues around the sample. The experiments were performed in six replicates, twelve of each sample were implanted. The changes in surface morphology of polymer samples after acute and chronic stages were examined by SEM. Besides, blood samples were taken from the animals and blood urea nitrogen (BUN) and creatinine (CR) values were measured.

2.12. Histological analysis

For histological analysis, at the end of acute and chronic *in vivo* biocompatibility studies, the tissues surrounding the implant were removed and immediately fixed in 10% formaldehyde. After the fixation, the tissues were washed in running tap water and then were dehydrated in alcohol, after which they were embedded in paraffin. The sections 4–5 μm thick from paraffin blocks were stained with hematoxylin-eosin (H-E), periodic acid schiff (PAS), toluidine blue (TM) and Masson trichrome (MT) to determine lymphocyte, macrophage, mast cell, and collagen density, respectively. Mast cell, lymphocyte and macrophage density was scored in 10 randomly selected areas as 0: none, 1: mild, 2: moderate, 3: severe. The intensity of staining in each image was calculated with the Image J image analysis program (National Institutes of Health, Bethesda, MD, USA). All analyzes and image acquisitions were performed using the Leica DFC-280 research microscope and the Leica Q Win Image Analysis System (Leica Micros Imaging Solutions Ltd., Cambridge, UK).

2.13. Biochemical analysis

Myeloperoxidase (MPO) and nitrite oxide (NO) parameters have been used in many studies in the literature as inflammation parameters [28]. Therefore, inflammation parameters of tissue samples were determined biochemically by MPO activity [29] and NO level [22].

2.14. Statistical analysis

Statistical analyzes for *in vitro* studies were performed with the GraphPad Prism 8 program (GraphPad Software, Inc., CA, US) by using One-way ANOVA test while statistical analyzes for histological studies were performed using IBM SPSS statistical software program (SPSS for Windows version 22, SPSS Inc., Chicago, IL). Comparison between groups, Anova (Tamhane or Tukey) test for data with normal distribution; Kruskal-Wallis H test was used for data that did not show normal distribution. Data were expressed as median (minimum-maximum) or arithmetic mean ± standard deviation depending on the distribution. When $p < 0.05$ the finding was considered statistically significant.

3. Results and discussion

In the present study, the polyurethane-acrylate formulations as a promising potential bone adhesive were synthesized, characterized, investigated of their *in vitro*, and *in vivo* biological activities. The structural and thermal characterizations and SEM and AFM results of these formulations are presented as “Supporting data”.

3.1. SEM and AFM results

The surface morphologies of the as-synthesized adhesives were determined by SEM analysis and the obtained images are presented in Fig. S53. From the image, it is clearly seen that the as-synthesized adhesive formulations were quite homogeneous, and smooth. The smooth structure indicating the good film formation after crosslinking of free

acrylate groups. In addition, the surface morphologies of the adhesives were examined by the AFM (Fig. S54). AFM results indicated that the surface roughness was below 250 nm for IPDI-GEL-P400 (~50 nm) and IPDI-COL-P400 (~250 nm) structures, but the IPDI-COL-P400 sample displayed a rougher structure compared to the other. The possible reason for this is that the formulations synthesized with collagen protein form a rougher structure. This nano-rough structure provides higher penetration of the adhesive into the tissue [30]. Finally, SEM and AFM

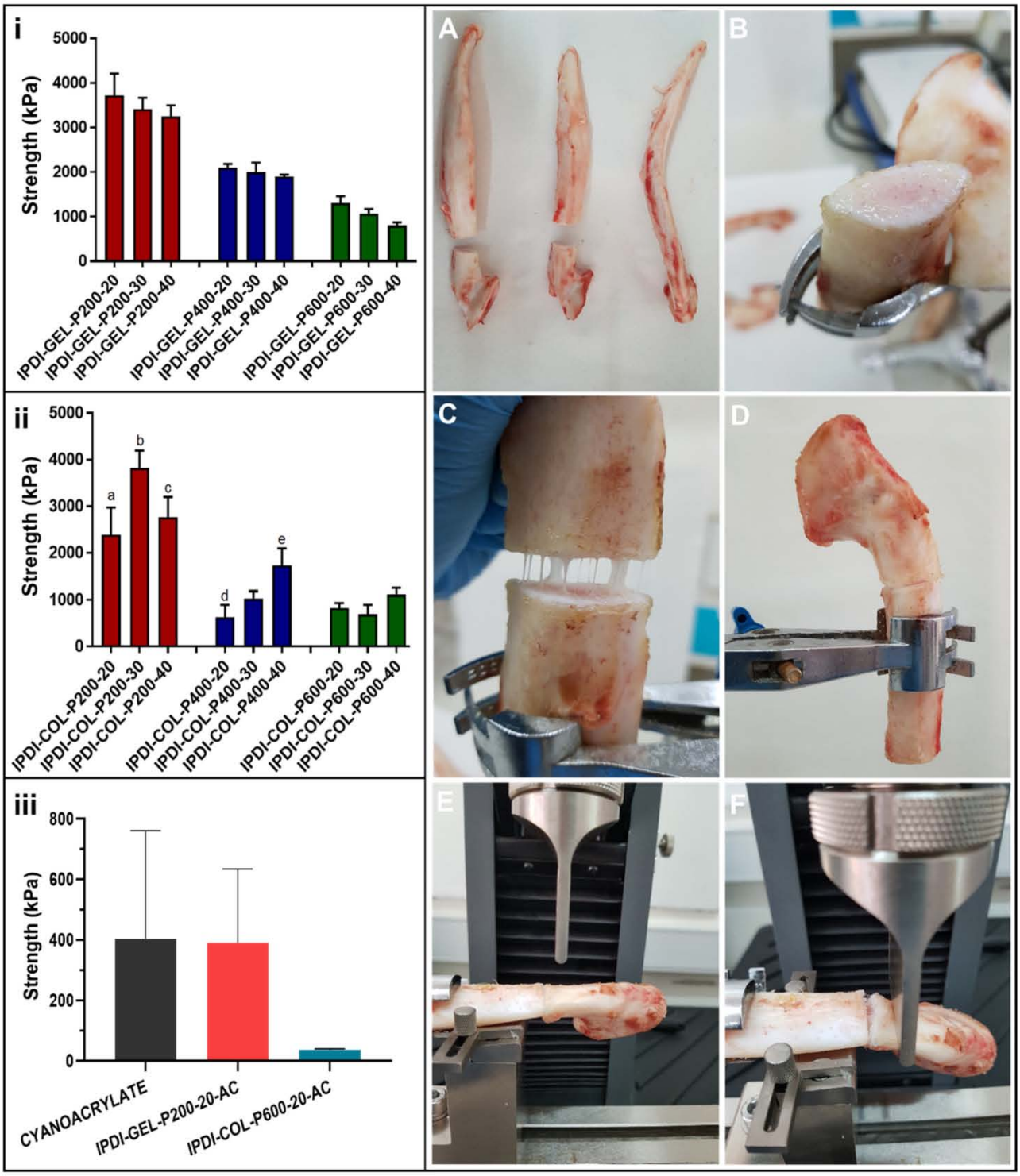

Fig. 2. Adhesive test results for (i) IPDI-GEL-PEG based formulations, and (ii) IPDI-COL-PEG based formulations in glass substrate.*Letters $p < 0.05$: a; IPDI-COL-P200-20 *vs* [IPDI-COL-P200-30, IPDI-COL-P400-20, IPDI-COL-P400-30, IPDI-COL-P600-20, IPDI-COL-P600-30, IPDI-COL-P600-40]; b; IPDI-COL-P200-30 *vs* [IPDI-COL-P400-20, IPDI-COL-P400-30, IPDI-COL-P400-40, IPDI-COL-P600-20, IPDI-COL-P600-30, IPDI-COL-P600-40]; c; IPDI-COL-P200-40 *vs* [IPDI-COL-P400-20, IPDI-COL-P400-30, IPDI-COL-P600-20, IPDI-COL-P600-30, IPDI-COL-P600-40]; d; IPDI-COL-P400-20 *vs* [IPDI-COL-P400-40]; e; IPDI-COL-P400-40 *vs* [IPDI-COL-P600-30]. (iii) represents *ex vivo* compressive strength analysis results. (A-F) represents the photographs of the preparation of the compression strength studies. (A) Bone tissues taken from the bovine rib area, (B) the cut tissue, (C) the application of adhesive formulations, (D) the curing with UV, (E) the placement of tissue in mechanical test analyzer, and (F) the application of compression strength.

analysis displayed very similar results.

3.2. Adhesion strength and ex vivo compressive strength analysis

Fig. 2(i) comparatively displays the adhesive strength analysis results in kPa of the adhesive formulations containing IPDI-GEL and different PEGs. According to our results, the adhesive formulations containing the PEG200 monomer showed the highest adhesive strength. The adhesive strength values of IPDI-GEL-P200-20, IPDI-GEL-P200-30, and IPDI-GEL-P200-40 samples were 3722.2 ± 486.8, 3410.7 ± 256.4., and 3250.7 ± 246.7 kPa, respectively. The adhesive strength results for the formulations containing PEG400 and PEG600 were measured in the range of 2010–1900 kPa and 800–1300 kPa, respectively. A change in bonding strength due to the increase in NCO:OH ratio is not statistically significant ($p > 0.05$). All breakages of GEL-based formulations occurred as adhesion/cohesion failure.

Fig. 2(ii) shows the adhesive strength of the adhesive the formulations containing IPDI-COL-PEG. According to the results, the adhesive strength results were measured in the range of 2389–3821 kPa, 631–1732 kPa and 692–1113 kPa for IPDI-COL-P200, IPDI-COL-P400 and IPDI-COL-P600, respectively. In general, a decrease in adhesive strength was observed with increasing molecular weight of PEG in the adhesive formulation. Also, the adhesive strength difference of these samples was found to be statistically significant ($p < 0.05$). All breakages of COL-based formulations occurred as adhesion/cohesion failure.

As seen in Fig. 3, PEG200-based polymers are relatively more rigid because they have more crosslink density, while PEG600-based polymers are more flexible due to less frequent crosslinks. In the study, three different molecular weights of PEG (200, 400, and 600) were used as chain extenders. When PEG structures are analyzed as monomers, PEG600 has the highest viscosity because it has the largest molecular weight, while PEG200 is the most fluid. On the contrary, as seen in the Fig. 3, when were used in PU synthesis, PEG200 formed more viscous pre-polymer as it has more dense crosslink points than the PEG600-based pre-polymer. In the final polyurethane-acrylates, the hardest structures were determined as the PEG200 containing polymers while the most flexible ones were found to be PEG600. For this reason, PEG200-based polymers showed the highest adhesion strength, while PEG600-based polymers, in contrast, showed the lowest strength.

Bhagat et al. developed polyester-(urea) based bone glue and achieved 1200 kPa adhesion strength on aluminum substrate [31]. In a most recent study, an acrylate-based adhesive was developed by Xiong et al., and the adhesion strength was measured as 2000 kPa on glass substrates [32]. Harper et al. produced photo-crosslinkable terpolymer adhesives and obtained ~1677 kPa adhesion strength after 5 min of UV curing [33]. Back et al. synthesized acrylic-based adhesives and obtained adhesion strength between 189 and 254 kPa [34]. Accordingly, adhesion strength of prepared adhesives is much higher than reference values [31–34].

After this stage of the study, IPDI-GEL-P200-20-AC and IPDI-COL-P600-20-AC formulations with the highest adhesion strength and ease of application were selected from 18 adhesive formulations for further analysis.

The photographs of the application of the compression strength studies are presented in Fig. 2(A–F). The *ex vivo* compression strength test was performed on bovine ribs using the selected formulations and a commercial adhesive product, VenaBlock embolization agent (cyanoacrylate). According to the results shown in Fig. 2(iii), the cyanoacrylate and IPDI-GEL-P200-20-AC samples showed similar strength as 403.4 and 390.1 kPa, respectively. However, there was no statistically significant difference between these two groups. On the other hand, the IPDI-COL-P600-20-AC formulation showed the lowest compression strength with a value of 36.8 kPa. This may be due to the PEG600 structure, which includes the low adhesive strength. The adhesion strength of IPDI-GEL-P200-20-AC (390 kPa) is comparable to commercially available product (cyanoacrylate, 403 kPa) and previously reported bone adhesives [31,35,36].

3.3. Biodegradability, gentamicin release and antibacterial activity studies

It is desirable that the prepared polyurethane-acrylate materials should have a biodegradable character as well as strong adhesive properties. It is well known that the monomers involved in the design of bioadhesive formulations significantly affect the degradation process and rate of degradation. According to our biodegradability results, a weight loss in the range of 20–40% was observed at the end of four weeks (Fig. 4A). Although the biodegradability rate of the formulations has changed, the highest mass loss was observed in the 1st week for all samples. Besides, it is clear from our results that an important parameter in the biodegradability of the formulations obtained is the weight of the molecule of the PEG units. The degradability of the formulation containing PEG200 was lower than that of PEG600. As a reason, it can be suggested that the cross-linking rate in the structure increases and the structure gains hardness depending on the molecular weight of the PEG. Our findings were similar to those of Sarkar et al. [37]. They reported that the molecular weight of PEG has a vital role on both the rate and extent of degradation of the polyether urethane samples. They observed in their findings that the rate and degree of degradation of polyether urethane samples increased with increasing molecular weight of PEG. In addition, our data observed were in line with what reported by Qian et al. [38].

Gentamicin-based biomaterials are used for local antibiotic effect [39]. The release of gentamicin from the formulations was analyzed by measuring the concentration of the gentamicin-OPA complex in PBS medium. The cumulative release profile of gentamicin from IPDI-GEL-P200-20-AC and IPDI-COL-P600-20-AC are illustrated in Fig. 4B. As we can observe, for the IPDI-GEL-P200-20-AC formulation, a rapid initial release (26.6% after 4 h soaking) followed by slower release of the gentamicin (to 28.6% after 24 h) occurred. A similar gentamicin release profile was observed in the IPDI-COL-P600-20-AC formulation. From this formulation, gentamicin was released 44.9% after 4 h of soaking while its release reached plateau level after 24 h. Besides, the gentamicin concentration in the PBS did not change significantly between 24 h and 120 h. The release results obtained are consistent with the aforementioned biodegradability results. As expected, the release of gentamicin from the IPDI-COL-P600-20-AC formulation increased, because the IPDI-COL-P600-20-AC formulation exhibited higher weight loss in the *in vitro* hydrolytic degradation test.

Agar disc diffusion method was tested to determine the antimicrobial effects of the adhesive formulations, and pure gentamicin was used as positive control. As seen in Fig. 4C and D, the formulations showed

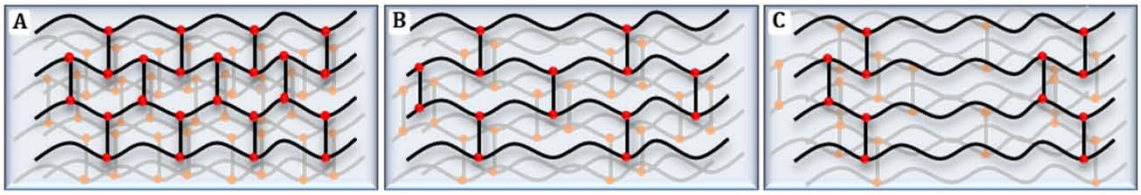

Fig. 3. Crosslinking density of PEG200 (A), PEG400 (B) and PEG600 (C)-based formulations.

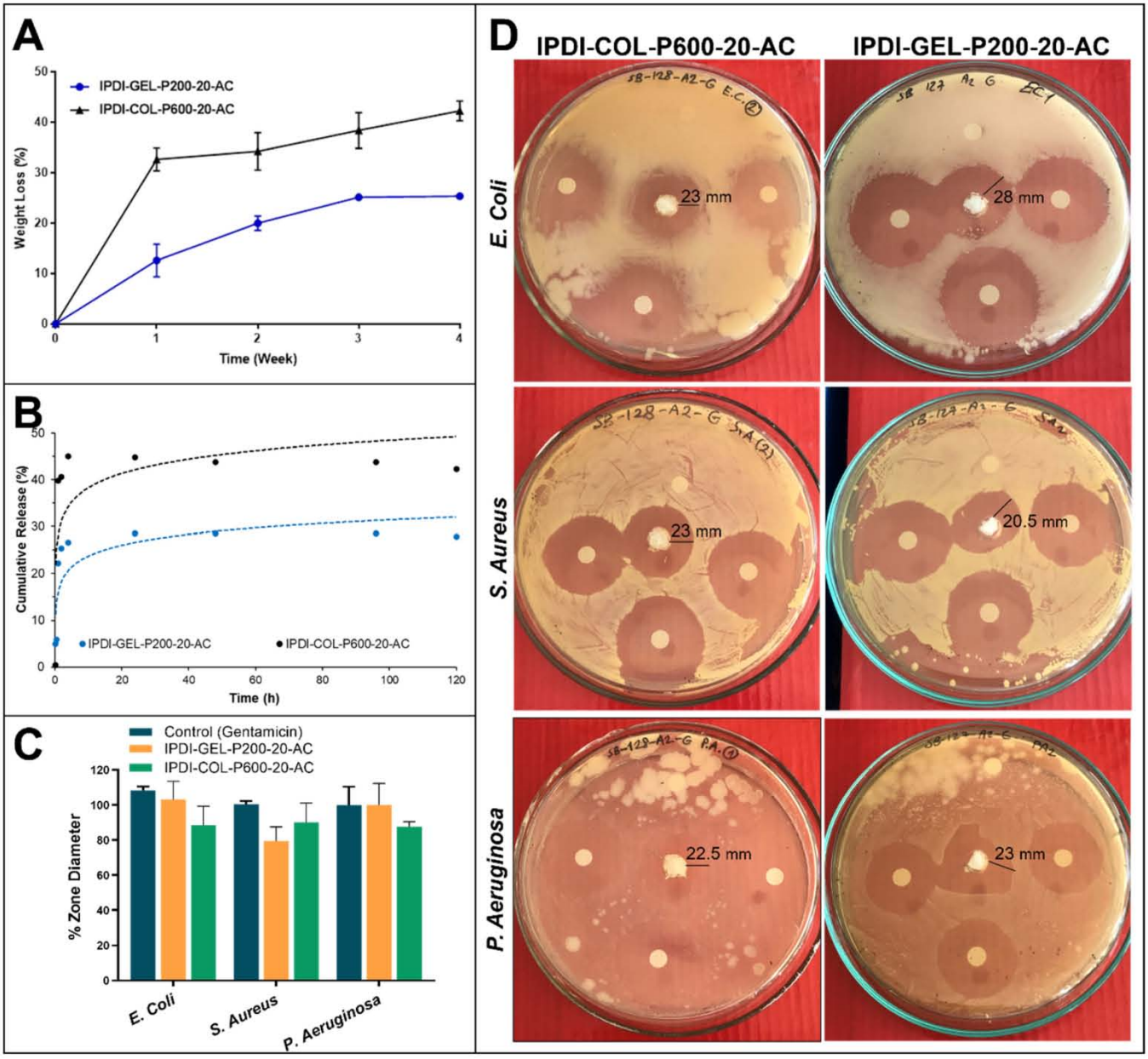

Fig. 4. The *in vitro* hydrolytic degradation results (A) and the cumulative gentamicin releasing results (B) of IPDI-GEL-P200-20-AC and IPDI-COL-P600-20-AC. % zone diameters (C) and zone diameters photographs of the adhesive formulations on *E. coli*, *S. aureus* and *P. aeruginosa* bacteria (D).

approximately 90% gentamicin equivalent activity. In particular, the zone diameters for *S. aureus* bacteria were very clear. Compared to the formulations, the IPDI-GEL-P200-20-AC showed higher bactericidal effects in Gram-bacteria species (*E. coli* and *P. Aeruginosa*), however, it was not statistically significant ($p > 0.05$). In addition, IPDI-COL-P600-20-AC displayed higher antibacterial effect in *S. aureus* bacterium, whereas it was not statistically significant ($p > 0.05$). Both of the formulations exhibited similar antibacterial activity, confirming that gentamicin was incorporated homogeneously and adequately into the formulations. Kimna et al. absorbed 0.2% gentamicin into the zein-based electrospun mats and they obtained 42% and 43% antimicrobial activity for *E. Coli* and *S. Aureus*, respectively [40]. Sohail et al. investigated the antimicrobial effect of lyophilized extracellular matrix envelope, hydrated in 40 mg/mL gentamicin, on methicillin-resistant *S. aureus*, *E. coli*, *P. aeruginosa*, and *S. marcescens*. According to their results, the envelope had killed all of the bacteria after 12 h [41]. As a result, the antibacterial activity of our formulations was comparable with the literature.

3.4. Protein adsorption

BSA and fibrinogen adsorption was carried out for the formulations prepared. BSA adsorption amounts were measured as 14.0 ± 12.0, and 57.4 ± 11.1 μg BSA/0.1 g sample for IPDI-GEL-P200-20-AC, and IPDI-COL-P600-20-AC, respectively. On the other hand, fibrinogen adsorption amounts were measured 21.2 ± 6.6, and 70.4 ± 7.6 μg fibrinogen/0.1 g sample for IPDI-GEL-P200-20-AC, and IPDI-COL-P600-20-AC, respectively. The fibrinogen adsorption values of the formulations were found very close to BSA adsorption. These results indicate that the adhesive formulations do not have special adsorption against fibrinogen.

3.5. In vitro biocompatibility

The *in vitro* biocompatibility results of the formulations performed by

the indirect method are presented in Fig. 5. According to the results, IPDI-COL-P600-20-AC formulation had higher cell viability than IPDI-GEL-P200-20-AC formulation. The cell viability values were observed to be about 85%, and about 99% for the IPDI-GEL-P200-20-AC, and the IPDI-COL-P600-20-AC, respectively. In addition, Fig. 6 (in the top left) shows the % confluent ratio of cells treated with formulations (n = 8) calculated by invert based counting system. The counts calculated from random wells confirmed the MTT results, but the difference was not statistically significant ($p > 0.05$). Moreover, according to the cell morphology images seen in Fig. 5 (top right and bottom), no change in morphology was observed and images close to control were obtained. The cell viability level here can be interpreted as a decrease in proliferation compared to the control. In the MTT test, the material is considered non-cytotoxic if the percentage of viable cell is greater than 70% of the untreated control according to ISO-10993-5. The results showed that the adhesive has sufficient biocompatibility.

3.6. *In vivo* biocompatibility

To investigate the *in vivo* biocompatibility of the formulations, histological and biochemical analyzes were performed by taking the muscle tissue surrounding the adhesive formulations at the end of the 1st and 4th week. When animals were sacrificed at the end of the 1st and 4th week to remove the muscle tissues, it was determined that the adhesive formulations were encapsulated by the subcutaneous tissue but there was no visible inflammation (Fig. 6A). No signs of physical disorder or behavioral change suggesting systemic or neurological toxicity were observed during the postoperative examinations. These results are consistent with histology results [42].

In *in vivo* biocompatibility experiments, SEM images of the IPDI-GEL-P200-20-AC and IPDI-COL-P600-20-AC formulations implanted in rats were taken before and 1 week and 4 weeks after implantation. As can be seen in Fig. 6B, all formulations were relatively flat and non-porous before implantation. In the 1st week, slight cracking started on the surfaces especially in the IPDI-GEL-P200-20-AC sample. In the 4th week, these cracks became more pronounced. This is an indication that the degradation process of the samples has begun. However, there was no visible morphology change in the IPDI-COL-P600-20-AC sample. The low rate of degradation of the samples may be due to rat muscle tissues encapsulating the samples.

3.7. *Histological analysis*

After the animals were sacrificed, at the end of the 1st and 4th week (acute and chronic), the tissues surrounding the adhesive formulations were removed and lymphocyte, macrophage and mast cell density were evaluated in order to determine the possible inflammatory effects of the adhesive formulations. Accordingly, mild inflammatory reaction was observed in all groups (including the control group), both acute and chronic. As a result of the evaluations, it was observed that the mast cells observed especially around the vessels and nerves were in similar density in all groups ($p > 0.05$, Fig. 7A). On the other hand, in terms of lymphocyte density, PP (Polypropylene) and IPDI-GEL-P200-20-AC groups were found to be statistically similar in both acute and chronic

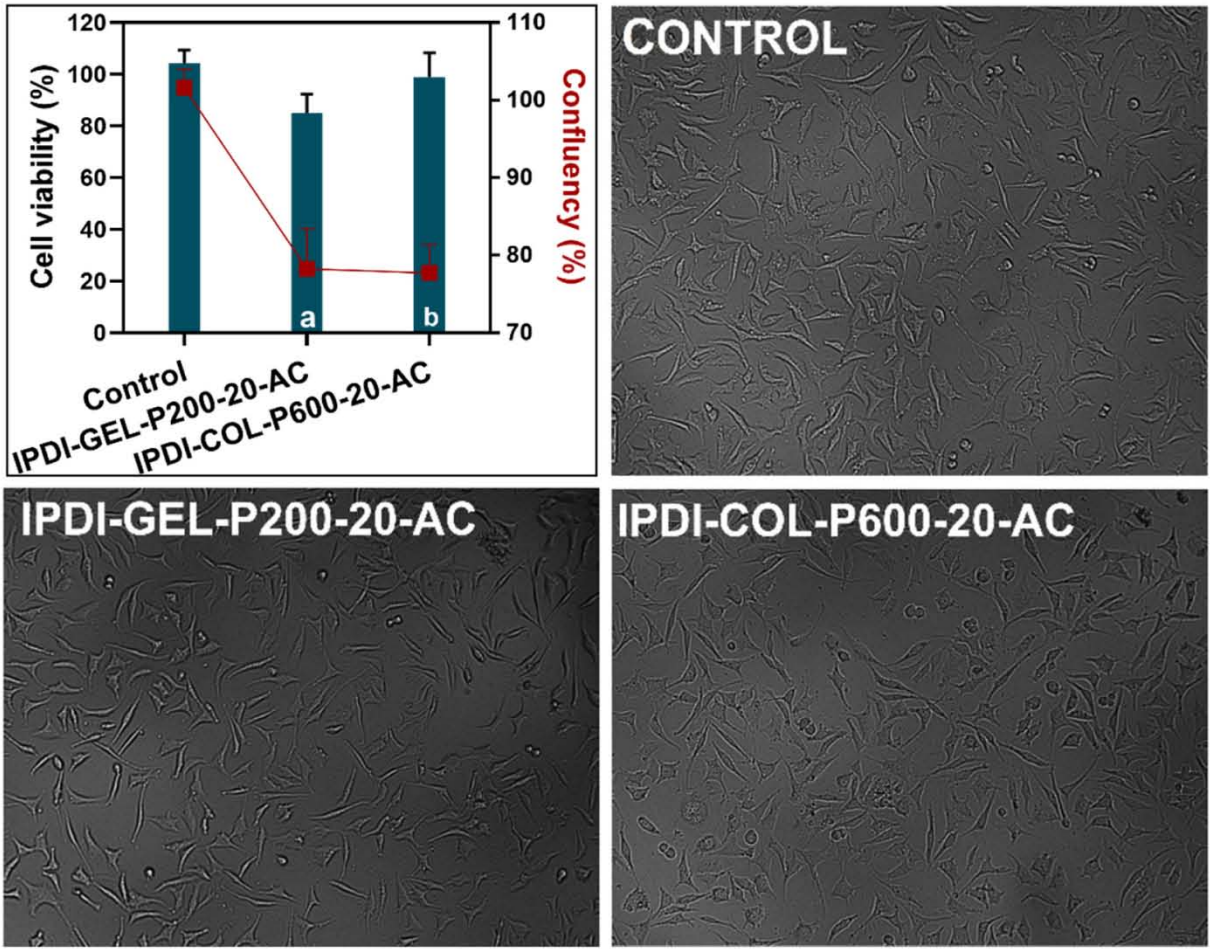

Fig. 5. In the top left; cell viability (column) and confluent (point) values of adhesive formulations on L-929 cells. The letters indicate results significant at $p < 0.05$: a represents significant compared to control; b represents statistical analysis for group comparison. In the top right and bottom; the morphological effects of the adhesive formulations on L-929 cells.

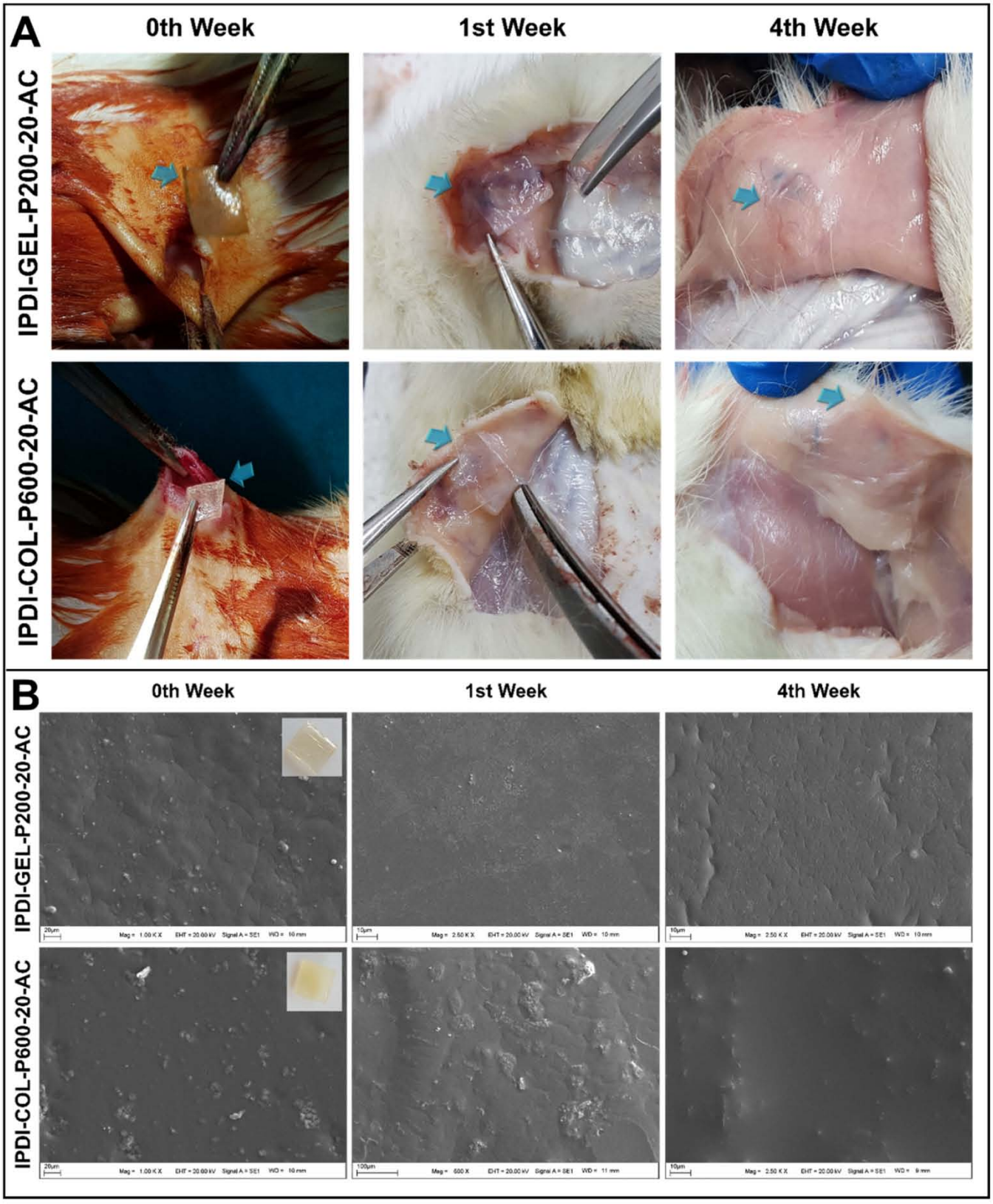

Fig. 6. (A); illustration of the interactions of the adhesive formulations with tissue at 0, 1 (acute) and 4 (chronic) weeks for *in vivo* biocompatibility test. (B); SEM images of the formulations implanted in rats at 0, 1 and 4 weeks.

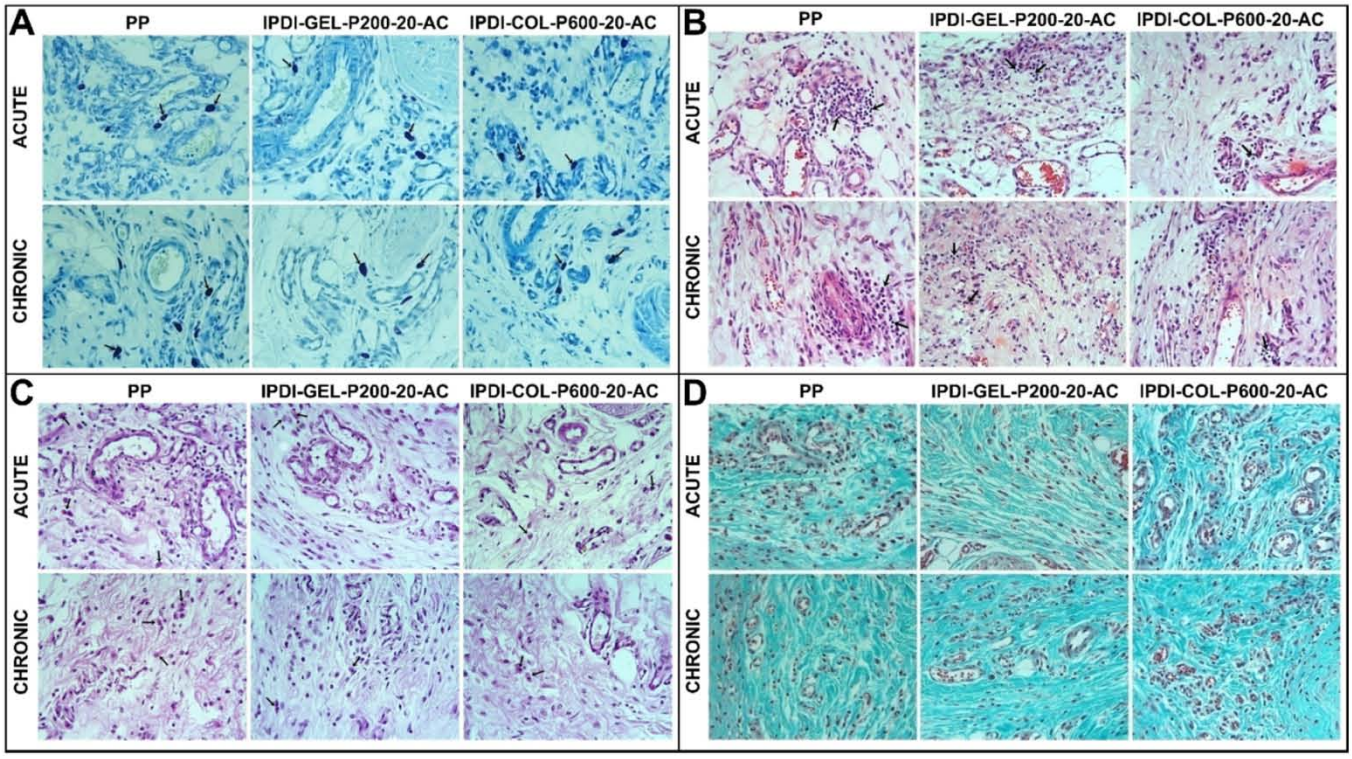

Fig. 7. (A); Mast cells (arrows) are observed around the vessels and nerves. TM; ×40. (B); Mild lymphocyte infiltration (arrows) observed in places as diffuse or foci. H-E; ×40. (C); Macrophages (arrows) traced in connective tissue. PAS; ×40. (D); A significant increase in collagen density (green area) in chronic groups is noticeable compared to the acute groups. MT; ×40.

applications ($p > 0.05$); It was found that the lymphocyte density in the IPDI-COL-P600-20-AC group was significantly lower than in the PP group ($p < 0.05$, Fig. 7B). Macrophage density was found to be statistically significantly lower in the acute and chronic IPDI-GEL-P200-20-AC and IPDI-COL-P600-20-AC groups compared to the PP group ($p < 0.05$, Fig. 7C). In the evaluations for collagen density, it was observed that acute and chronic groups had statistically similar collagen density within themselves ($p > 0.05$, Fig. 7D). On the other hand, it was noted that the collagen density measured in chronic groups was higher than in acute groups. Histological evaluation results are given in Table 2, and comparison results between groups (p values) are given in Table S1.

Table 2
The histological evaluation results for *in vivo* biocompatibility assay.

	Mast cell density		Lymphocyte density	
Groups	Acute	Chronic	Acute	Chronic
PP	1.0 (0.0–3.0)	1.0 (0.0–3.0)	1.0 (0.0–2.0)	1.0 (0.0–2.0)
IPDI-GEL-P200-20-AC	1.0 (0.0–2.0)	1.0 (0.0–3.0)	1.0 (0.0–2.0)	1.0 (0.0–2.0)
IPDI-COL-P600-20-AC	1.0 (0.0–3.0)	2.0 (0.0–3.0)	0.0 (0.0–2.0)[a]	0.0 (0.0–2.0)[b]

	Macrophage density		Collagen density	
Groups	Acute	Chronic	Acute	Chronic
PP	1.0 (0.0–3.0)	1.0 (0.0–3.0)	40.92 ± 11.08	54.86 ± 10.73
IPDI-GEL-P200-20-AC	0.0 (0.0–3.0)[a]	1.0 (0.0–3.0)[b]	36.65 ± 8.12	52.36 ± 9.26
IPDI-COL-P600-20-AC	0.0 (0.0–3.0)[a]	1.0 (0.0–3.0)[b]	41.91 ± 9.06	55.57 ± 9.04

[a] Significantly lower than acute control group ($p < 0.05$).
[b] Significantly lower than the chronic control group ($p < 0.05$).

3.8. Biochemical analyses

After the *in vivo* biocompatibility test, MPO analysis was performed on the tissues taken from the environment of the adhesive formulations. According to the results shown in Fig. 8A, when the acute and chronic groups were compared within themselves, there was no significant difference between the groups ($p > 0.05$). It is well known that MPO ratio increases in tissues due to inflammation [43]. There was no significant difference between any group after the experiment and the results were similar to the control (PP) prove that the adhesive formulations did not cause inflammation in the acute and chronic processes.

According to the NO results shown in Fig. 8B, there is no statistically significant change between groups in both acute and chronic applications. These results are consistent with MPO and histological results in terms of inflammation parameters.

BUN and CR levels were determined in terms of evaluating the kidney functions as a result of biodegradation of the adhesive formulations embedded in the back of serum samples obtained from rats. According to the results obtained, BUN and CR levels were similar in all groups (Fig. 8C and D). These results confirm that our formulations have no effect on BUN and CR levels on kidney function after biodegradation. These results support that the adhesive formulations developed were biocompatible.

4. Conclusions

Here, we report a novel bone tissue adhesive using acrylate functionalized polyurethane as the base formulation and gentamicin as the antibacterial agent to improve hard tissue adhesion. Adhesive character of the formulations was achieved by curing acrylate groups *via* UV irradiation. We characterized by using various techniques their chemical structure, thermal stability, mechanical properties, and microstructure. By incorporation of gentamicin, the adhesive formulations showed improved antibacterial activity toward bacterial strains. *In vitro* and *ex*

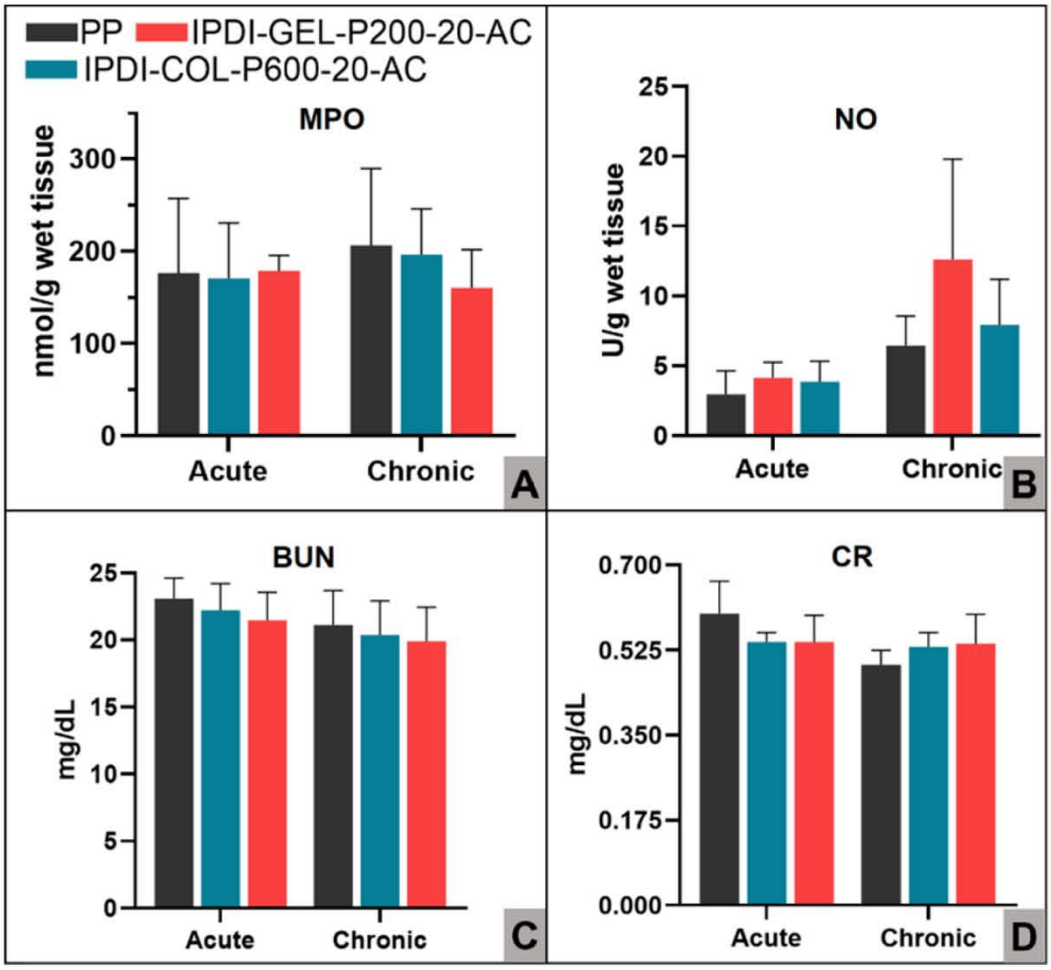

Fig. 8. (A) MPO; (B) NO; (C) BUN and (D) CR levels of the adhesive formulations in acute and chronic process.

vivo tests revealed that these adhesive formulations have excellent adhesive properties. Furthermore, the adhesive formulations could be degraded and absorbed *in vivo*, and displayed good cell compatibility. Finally, we also demonstrated the biocompatibility of the adhesive formulations over 4 weeks through *in vivo* tests in rat. Taken together, these results demonstrated that the synthesized adhesive formulations can be used not only for soft tissue but also for bone adhesives due to high performance. In future studies, we will focus on *in vivo* evaluations to confirm the potential of these adhesive formulations in bone tissue engineering applications.

CRediT authorship contribution statement

Sevgi Balcioglu (Corresponding A. 2); Conceptualization, Methodology, Software, Validation, Formal analysis, Investigation, Visualization, Writing - Review & Editing, Writing - Original Draft, Resources.

Canbolat Gurses; Formal analysis.

Imren Ozcan; Formal analysis.

Azibe Yildiz; Formal analysis.

Suleyman Koytepe; Term, Funding acquisition, Conceptualization, Methodology, Formal analysis, Investigation.

Hakan Parlakpinar; Formal analysis, Funding acquisition.

Nigar Vardi; Formal analysis, Funding acquisition.

Burhan Ates (Corresponding A. 1); Term, Project administration, Funding acquisition, Conceptualization, Methodology, Software, Validation, Formal analysis, Investigation, Visualization, Writing - Review & Editing, Writing - Original Draft, Resources.

Declaration of competing interest

The authors have no conflict of interest to declare.

Acknowledgements

This work was supported financially by the Scientific and Technological Research Council of Turkey [No. 116Z501] and Inonu University [No. FDP-2018-1284].

Appendix A. Supplementary data

Supplementary data to this article can be found online at https://doi.org/10.1016/j.ijbiomac.2021.09.043.

References

[1] B. Cohen, M. Panker, E. Zuckerman, M. Foox, M. Zilberman, Effect of calcium phosphate-based fillers on the structure and bonding strength of novel gelatin-alginate bioadhesives, J. Biomater. Appl. 28 (2014) 1366–1375, https://doi.org/10.1177/0885328213509502.

[2] Y. Liu, Z. Zhu, X. Pei, X. Zhang, X. Cheng, S. Hu, X. Gao, J. Wang, J. Chen, Q. Wan, ZIF-8-modified multifunctional bone-adhesive hydrogels promoting angiogenesis and osteogenesis for bone regeneration, ACS Appl. Mater. Interfaces 12 (2020) 36978–36995, https://doi.org/10.1021/acsami.0c12090.

[3] M.S. Desai, M. Chen, F.H.J. Hong, J.H. Lee, Y. Wu, S.W. Lee, Catechol-functionalized elastin-like polypeptides as tissue adhesives, Biomacromolecules. 21 (2020) 2938–2948, https://doi.org/10.1021/acs.biomac.0c00740.

[4] A. Kirillova, O. Nillissen, S. Liu, C. Kelly, K. Gall, Reinforcement and fatigue of a bioinspired mineral–organic bioresorbable bone adhesive, Adv. Healthc. Mater. 10 (2021) 2001058, https://doi.org/10.1002/adhm.202001058.

[5] K. Fujii, A. Lai, N. Korda, W.W. Hom, T.W. Evashwick-Rogler, P. Nasser, A. C. Hecht, J.C. Iatridis, Ex-vivo biomechanics of repaired rat intervertebral discs using genipin crosslinked fibrin adhesive hydrogel, J. Biomech. 113 (2020), https://doi.org/10.1016/j.jbiomech.2020.110100.
[6] P.A. Leggat, D.R. Smith, U. Kedjarune, Surgical applications of cyanoacrylate adhesives: a review of toxicity, ANZ J. Surg. 77 (2007) 209–213, https://doi.org/10.1111/j.1445-2197.2007.04020.x.
[7] H. Yan, L. Li, Z. Wang, Y. Wang, M. Guo, X. Shi, J.M. Yeh, P. Zhang, Mussel-inspired conducting copolymer with aniline tetramer as intelligent biological adhesive for bone tissue engineering, ACS Biomater Sci. Eng. 6 (2020) 634–646, https://doi.org/10.1021/acsbiomaterials.9b01601.
[8] Q. Zhang, C. Huang, H. Wang, M. Hu, H. Li, X. Liu, UV-curable coating crosslinked by a novel hyperbranched polyurethane acrylate with excellent mechanical properties and hardness †, 2016, https://doi.org/10.1039/c6ra21081c.
[9] H. Sugita, K. Itou, Y. Itou, N. Wada, T.U. Shin-ya Kurita, Y. Hirose, K. Hatase, H. Matsumoto, D. Ichinohe, Multi-acrylate-based UV-curable dismantlable adhesives, Int. J. Adhes. Adhes. 104 (2021), https://doi.org/10.1016/j.ijadhadh.2020.102758.
[10] T. Cernadas, M. Santos, F.A.M.M. Gonçalves, P. Alves, T.R. Correia, I.J. Correia, P. Ferreira, Functionalized polyester-based materials as UV curable adhesives, Eur. Polym. J. 120 (2019), https://doi.org/10.1016/j.eurpolymj.2019.08.023.
[11] R.S. Mishra, A.K. Mishra, K.V.S.N. Raju, Synthesis and property study of UV-curable hyperbranched polyurethane acrylate/ZnO hybrid coatings, Eur. Polym. J. 45 (2009) 960–966, https://doi.org/10.1016/j.eurpolymj.2008.11.023.
[12] H. Chen, S.Y. Lee, Y.M. Lin, Synthesis and formulation of PCL-based urethane acrylates for DLP 3D printers, Polymers 12 (2020) 1–17, https://doi.org/10.3390/polym12071500.
[13] M. Zhang, Y.-D. Meng, H.-W. Li, H.-W. Li, Curing Behavior of the UV-curable Cationic Waterborne Polyurethane Acrylate Adhesives, World Scientific Pub Co Pte Lt, 2016, pp. 507–515, https://doi.org/10.1142/9789813143401_0057.
[14] S.W. Lee, J.W. Park, C.H. Park, D.H. Lim, H.J. Kim, J.Y. Song, J.H. Lee, UV-curing and thermal stability of dual curable urethane epoxy adhesives for temporary bonding in 3D multi-chip package process, Int. J. Adhes. Adhes. 44 (2013) 138–143, https://doi.org/10.1016/j.ijadhadh.2013.02.005.
[15] H.S. Joo, Y.J. Park, H.S. Do, H.J. Kim, S.Y. Song, K.Y. Choi, The curing performance of UV-curable semi-interpenetrating polymer network structured acrylic pressure-sensitive adhesives, J. Adhes. Sci. Technol. 21 (2007) 575–588, https://doi.org/10.1163/156856107781192346.
[16] M.D. Shoulders, R.T. Raines, Collagen structure and stability, Annu. Rev. Biochem. 78 (2009) 929–958, https://doi.org/10.1146/annurev.biochem.77.032207.120833.
[17] Z. Bai, W. Dan, G. Yu, Y. Wang, Y. Chen, Y. Huang, C. Yang, N. Dan, Tough and tissue-adhesive polyacrylamide/collagen hydrogel with dopamine-grafted oxidized sodium alginate as crosslinker for cutaneous wound healing, RSC Adv. 8 (2018) 42123–42132, https://doi.org/10.1039/c8ra07697a.
[18] A.R. Del Bakhshayesh, N. Asadi, A. Alihemmati, H. Tayefi Nasrabadi, A. Montaseri, S. Davaran, S. Saghati, A. Akbarzadeh, A. Abedelahi, An overview of advanced biocompatible and biomimetic materials for creation of replacement structures in the musculoskeletal systems: focusing on cartilage tissue engineering, J. Biol. Eng. 13 (2019) 1–21, https://doi.org/10.1186/s13036-019-0209-9.
[19] F. Öfkeli, D. Demir, N. Bölgen, Biomimetic mineralization of chitosan/gelatin cryogels and in vivo biocompatibility assessments for bone tissue engineering, J. Appl. Polym. Sci. 138 (2021), https://doi.org/10.1002/app.50337.
[20] S. Vedovatto, J.C. Facchini, R.K. Batista, T.C. Paim, M.I.Z. Lionzo, M.R. Wink, Development of chitosan, gelatin and liposome film and analysis of its biocompatibility in vitro, Int. J. Biol. Macromol. 160 (2020) 750–757, https://doi.org/10.1016/j.ijbiomac.2020.05.229.
[21] B. Ates, S. Koytepe, M.G. Karaaslan, S. Balcioglu, S. Gulgen, Biodegradable non-aromatic adhesive polyurethanes based on disaccharides for medical applications, Int. J. Adhes. Adhes. 49 (2014) 90–96, https://doi.org/10.1016/j.ijadhadh.2013.12.012.
[22] S. Balcioglu, H. Parlakpinar, N. Vardi, E.B. Denkbas, M.G. Karaaslan, S. Gulgen, E. Taslidere, S. Koytepe, B. Ates, Design of xylose-based semisynthetic polyurethane tissue adhesives with enhanced bioactivity properties, ACS Appl. Mater. Interfaces 8 (2016) 4456–4466, https://doi.org/10.1021/acsami.5b12279.
[23] B. Ates, S. Koytepe, M.G. Karaaslan, S. Balcioglu, S. Gulgen, M. Demirbilek, E. B. Denkbas, Chlorogenic acid containing bioinspired polyurethanes: biodegradable medical adhesive materials, Int. J. Polym. Mater. Polym. Biomater. 64 (2015) 611–619, https://doi.org/10.1080/00914037.2014.996710.
[24] B. Ates, S. Koytepe, S. Balcioglu, M.G. Karaaslan, U. Kelestemur, S. Gulgen, O. Ozhan, Biomimetic approach to tunable adhesion of polyurethane adhesives through Fe3+ crosslinking and hydrophobic tween units with balance of adhesion/cohesion forces, Int. J. Adhes. Adhes. 95 (2019) 102396, https://doi.org/10.1016/j.ijadhadh.2019.102396.
[25] Y. Chang, C.-L. Tai, P.-H. Hsieh, S.W.N. Ueng, Gentamicin in bone cement, Bone Joint Res. 2 (2013) 220–226, https://doi.org/10.1302/2046-3758.210.2000188.
[26] A.I. Al-Amoud, B.J. Clark, H. Chrystyn, Determination of gentamicin in urine samples after inhalation by reversed-phase high-performance liquid chromatography using pre-column derivatisation with o-phthalaldehyde, J. Chromatogr. B Anal. Technol. Biomed. Life Sci. 769 (2002) 89–95, https://doi.org/10.1016/S1570-0232(01)00636-5.
[27] A.W. Bauer, W.M. Kirby, J.C. Sherris, M. Turck, Antibiotic susceptibility testing by a standardized single disk method., Am. J. Clin. Pathol. (1966). doi:https://doi.org/10.1093/ajcp/45.4_ts.493.
[28] J.P. Eiserich, Leukocyte-derived Myeloperoxidase Is a Physiological Nitric Oxide and Nitrite Oxidase: Functions Beyond Host Defense, Springer, Dordrecht, 2003, pp. 121–135, https://doi.org/10.1007/978-94-007-0958-4_10.
[29] L.M. Hillegass, D.E. Griswold, B. Brickson, C. Albrightson-Winslow, Assessment of myeloperoxidase activity in whole rat kidney, J. Pharmacol. Methods 24 (1990) 285–295, https://doi.org/10.1016/0160-5402(90)90013-B.
[30] Y. Liu, X. Liu, M. Wu, P. Ji, H. Lv, L. Deng, A collagen film with micro-rough surface can promote the corneal epithelization process for corneal repair, Int. J. Biol. Macromol. 121 (2019) 233–238, https://doi.org/10.1016/J.IJBIOMAC.2018.10.026.
[31] V. Bhagat, E. O'Brien, J. Zhou, M.L. Becker, Caddisfly inspired phosphorylated poly (ester urea)-based degradable bone adhesives, Biomacromolecules. 17 (2016) 3016–3024, https://doi.org/10.1021/acs.biomac.6b00875.
[32] G. Xiong, W. Xiong, S. Dai, M. Lin, G. Xia, X. Wan, Y. Mu, Fast-curing mussel-inspired adhesive derived from vegetable oil, ACS Appl. Bio Mater. (2021), https://doi.org/10.1021/acsabm.0c01245.
[33] T. Harper, R. Slegeris, I. Pramudya, H. Chung, Single-phase photo-cross-linkable bioinspired adhesive for precise control of adhesion strength, ACS Appl. Mater. Interfaces 9 (2017) 1830–1839, https://doi.org/10.1021/ACSAMI.6B14599.
[34] J.-H. Back, Y. Kwon, J.C. Roldao, Y. Yu, H.-J. Kim, J. Gierschner, W. Lee, M. S. Kwon, Synthesis of solvent-free acrylic pressure-sensitive adhesives via visible-light-driven photocatalytic radical polymerization without additives, Green Chem. 22 (2020) 8289–8297, https://doi.org/10.1039/D0GC02807J.
[35] D. Lu, H. Wang, T. Li, Y. Li, X. Wang, P. Niu, H. Guo, S. Sun, X. Wang, X. Guan, H. Ma, Z. Lei, Versatile surgical adhesive and hemostatic materials: synthesis, properties, and application of thermoresponsive polypeptides, Chem. Mater. 29 (2017) 5493–5503, https://doi.org/10.1021/acs.chemmater.7b00255.
[36] H. Zhang, L. Bré, T. Zhao, B. Newland, M. Da Costa, W. Wang, A biomimetic hyperbranched poly(amino ester)-based nanocomposite as a tunable bone adhesive for sternal closure, J. Mater. Chem. B 2 (2014) 4067, https://doi.org/10.1039/c4tb00155a.
[37] S. Sarkar, P. Basak, B. Adhikari, Biodegradation of polyethylene glycol-based polyether urethanes, Polym.-Plast. Technol. Eng. 50 (2011) 80–88, https://doi.org/10.1080/03602559.2010.531415.
[38] Z.Y. Qian, S. Li, Y. He, X.B. Liu, Synthesis and in vitro degradation study of poly (ethylene terephthalate)/poly(ethylene glycol) (PET/PEG) multiblock copolymer, Polym. Degrad. Stab. 83 (2004) 93–100, https://doi.org/10.1016/S0141-3910(03)00229-5.
[39] A. Pradeep, J. Rangasamy, P.K. Varma, Recent developments in controlling sternal wound infection after cardiac surgery and measures to enhance sternal healing, Med. Res. Rev. (2020), med.21758, https://doi.org/10.1002/med.21758.
[40] C. Kimna, S. Tamburaci, F. Tihminlioglu, Novel zein-based multilayer wound dressing membranes with controlled release of gentamicin, J. Biomed. Mater. Res. B Appl. Biomater. 107 (2019) 2057–2070, https://doi.org/10.1002/jbm.b.34298.
[41] M.R. Sohail, Z. Esquer Garrigos, C.S. Elayi, K. Xiang, J.N. Catanzaro, Preclinical evaluation of efficacy and pharmacokinetics of gentamicin containing extracellular-matrix envelope, Pacing Clin. Electrophysiol. 43 (2020) 341–349, https://doi.org/10.1111/pace.13888.
[42] K.H. Sun, Z. Liu, C. Liu, T. Yu, T. Shang, C. Huang, M. Zhou, C. Liu, F. Ran, Y. Li, Y. Shi, L. Pan, Evaluation of in vitro and in vivo biocompatibility of a myo-inositol hexakisphosphate gelated polyaniline hydrogel in a rat model, Sci. Rep. 6 (2016) 1–11, https://doi.org/10.1038/srep23931.
[43] V. Loria, I. Dato, F. Graziani, L.M. Biasucci, Myeloperoxidase: a new biomarker of inflammation in ischemic heart disease and acute coronary syndromes, Mediat. Inflamm. 2008 (2008), https://doi.org/10.1155/2008/135625.